
AUTONOMOUS SEARCH OF AN AIRBORNE RELEASE IN URBAN ENVIRONMENTS USING INFORMED TREE PLANNING

A PREPRINT

Callum Rhodes

Dept. of Aeronautical and Automotive Engineering
Loughborough University
Loughborough, LE11 3TU, UK
c.rhodes@lboro.ac.uk

Cunjia Liu *

Dept. of Aeronautical and Automotive Engineering
Loughborough University
Loughborough, LE11 3TU, UK
c.liu5@lboro.ac.uk

Paul Westoby

CBR Division
Dstl Porton Down
Salisbury, SP4 0JQ, UK pbwestoby@dstl.gov.uk

Wen-Hua Chen

Dept. of Aeronautical and Automotive Engineering
Loughborough University
Loughborough, LE11 3TU, UK
w.chen@lboro.ac.uk

ABSTRACT

The use of autonomous vehicles for chemical source localisation is a key enabling tool for disaster response teams to safely and efficiently deal with chemical emergencies. Whilst much work has been performed on source localisation using autonomous systems, most previous works have assumed an open environment or employed simplistic obstacle avoidance, separate to the estimation procedure. In this paper, we explore the coupling of the path planning task for both source term estimation and obstacle avoidance in a holistic framework. The proposed system intelligently produces potential gas sampling locations based on the current estimation of the wind field and the local map. Then a tree search is performed to generate paths toward the estimated source location that traverse around any obstacles and still allow for exploration of potentially superior sampling locations. The proposed informed tree planning algorithm is then tested against the Entrotaxis technique in a series of high fidelity simulations. The proposed system is found to reduce source position error far more efficiently than Entrotaxis in a feature rich environment, whilst also exhibiting vastly more consistent and robust results.

Keywords source term estimation · path planning · environmental sampling · autonomous search · informed tree

1 Introduction

The quick acquisition of accurate estimates about the source of a Chemical, Biological, Radiological and Nuclear (CBRN) release is vital in the process of minimising the impact of the resulting hazard and allowing first responders to quickly manage the situation. Doing so with manual sensor probes puts human operators at a high risk of life threatening situations, especially when considering the state of such environments can be highly uncertain. To mitigate this risk, the use of mobile robotic sensors has seen increasing interest as they can be deployed quickly in areas that are inaccessible to humans [Murphy et al., 2012].

Whilst the use of manually driven CBRN robots has already seen use in the field, for example in settings such as nuclear plant decommissioning [Tsitsimpelis et al., 2019], these vehicles must be operated by trained users. If a trained operator is not available or close by at the onset of a disaster event, then the manual nature of the system adds further delay to a

*Corresponding author

process which is heavily time critical. The obvious next step to this problem is to automate the task of data collection, allowing robotic agents to be deployed autonomously.

When considering an autonomous system for a source search task, there are several basic functionalities that the agent needs to possess. Firstly, it should be able to estimate source term parameters as it collects data. This is so that the system can update its belief about the source and use this information to help dictate its next course of action, e.g. collecting data for recursive inference. Secondly, the agent should be able to plan valid trajectories to data sampling locations that help achieve the task of finding the source. This process in feature rich environments is denoted as informative path planning (IPP).

Many works, including the pioneering work by Ristic et al. [2016], have focused on the first task of source term estimation and only briefly incorporate some form of IPP thus having little appreciation to feature rich environments (which cannot be overlooked for real-world CBRN incidents). Most of the existing solutions also use a myopic path planner, so may limit the searching efficacy. Therefore, this paper seeks to develop an improved IPP solution to the source term estimation problem that is capable of navigating complex environments whilst efficiently carrying out its task of localising an unknown source.

It should be noted that although path planning in complex environments has generated solutions that consider long term trajectories and the overall goal of the agent in a wide array of scenarios, it is not straightforward to bring them into the source term estimation framework. Algorithms that use rapidly-exploring random trees (RRT) structure are popular in literature due to the flexibility on dynamic constraints, with their spanning trees capable of expanding into any free space. However, directly applying this free spanning feature may not produce good results in the case of a source search in an urban environment. It is intuitive that sampling downwind of buildings is less likely to achieve accurate concentration data than in the open wind direction. Therefore, more samples should be collected in preferential areas compared to obscured areas, so that analytic dispersion models can be used to interpret the measurements. This principle may be violated by the one-sample-per-batch approach of RRT as branches are grown heuristically towards a sampled state. Recent works on Fast marching trees (FMT*) [Janson et al., 2015] and batch informed trees (BIT*) [Gammell et al., 2015] are two sampling based approaches that sample the whole environment to create a random geometric graph (RGG) in which spanning trees are expanded. Such multi-sample batch methods allow a custom sampling distribution to be enforced and therefore a variant of this technique will be explored in the proposed informed tree approach.

Another requirement to be considered is the efficiency of the search, which requires a good balance between exploration and exploitation. The goal location in conventional path planner is specified in some way, so that it can be directly exploited. For example, in Gammell et al. [2015] the use of a goal set is postulated alongside the single goal state. When combining with a Bayesian inference framework to estimate the source location (i.e. navigation goal), there is not a single (or set) location, but instead it is described by a probability density function (PDF). To this end, inspired by the Dual Control principle introduced in Chen et al. [2020], the goal state used by the proposed informed tree search algorithm is modified, so that the tree can be spanned iteratively towards the source while accounting for the uncertainty of the source term estimation,

By addressing the above technical challenges, this paper develops a more powerful and more applicable IPP framework for searching an unknown CBRN source in an urban environment. This paper is organised as follows. In Section 2, relevant works are reviewed to justify the novelty of this work. Section 3 formulates the problem to be considered, followed by technical solutions in Sections 4 - 6. The proposed algorithm is tested and verified in Section 7 using a high fidelity dataset and the conclusions are provided in section 8.

2 State of the art

CBRN related robotics has seen a swell of research interest in recent years, as recently summarised in Monroy and Gonzalez-Jimenez [2019], due to the ever increasing computational capabilities of small onboard chipsets and chemical sensors that can be easily fitted to mobile platforms including small UAVs. Coupled with their mobility to collect large amounts of data at any location, these systems are highly beneficial compared to the traditional approach of sparse static sensors running alongside complex CFD models that can take several days to resolve. To enable these mobile systems for source localisation tasks, both online estimation and motion planning functions need to be developed.

2.1 Estimation

Probabilistic estimation algorithms can be split into two categories, i.e., using parametric models and non-parametric models. In parametric estimation algorithms, the PDF of the underlying parameters of the atmospheric transport and diffusion (ATD) model will be established. Examples of light-weight ATD models that have been applied to mobile

robots include the Gaussian plume (GP) model [Wang et al., 2018] and the isotropic plume (IP) model [Vergassola et al., 2007]. These models describe the expected concentration at a given location under defined source terms and environmental conditions. These simple models have drawbacks in that they make strong assumptions about the source (such as a single source, constant release and uniform wind fields), however their computational efficiency lends towards the inclusion in probabilistic frameworks.

Non-parametric models for gas localisation include Gaussian Process [Hutchinson et al., 2019a], Kernel DM+V [Lilienthal et al., 2009] and Gaussian Markov random fields [G. Monroy et al., 2016]. The number of parameters in these models is not fixed and therefore less assumptions are made about the gas distributions. To account for the transportation of particles, GMRF and Kernel DM have further additions to account for wind direction in GW-GMRF [Gongora et al., 2020] and Kernel DM+V/W [Asadi et al., 2017]. This leads to the ability to account for multi modal distributions and the inclusion of obstacles in the environment. A major drawback of these methods are that they are poor at estimating outside of sample locations and require a large and varied set of data to accurately estimate the distribution. For a source term estimation case, this leads to the case that if the area near the source location itself cannot be sampled (such may be the case in an urban environment), then non-parametric models tend to be unable to accurately estimate the source. Furthermore, these models tend to be computationally expensive to iteratively calculate. Note that the framework proposed in this paper can use both model types (e.g. Rhodes et al. [2020]), therefore leaving flexibility in the system. However, a parametric model is used in this work, not only due to its computational efficiency and wide spread adoption in the literature, but also because one of the motivations of this work is to show that such simple ATD models are adequate to inform robotic source localisation in urban environments, given features can be accommodated in the path planning algorithm.

2.2 Motion planning

Motion planning of mobile robots plays a key role in many IPP frameworks for environment monitoring. However, in the literature, motion planning for source search is generally limited to goal selection i.e., which place should be sampled next. To solve the goal selection problem that is inherent in an autonomous system, there are three classes of algorithms employed: coverage based, bio-inspired and information theoretic. Coverage based planners (e.g. Hombal et al. [2010], Galceran and Carreras [2013]) rely on predetermined trajectories to maximise coverage of the search area in a systematic manner. These algorithms are incredibly efficient and easy to implement but are decoupled from the estimation side of the system. Therefore, they can be ineffective and difficult to scale. Bio-inspired methods such as Anemotaxis [Harvey et al., 2008] and Chemotaxis [Dhariwal et al., 2004, Russell et al., 2003] use instantaneous concentration and anemometry measurements to guide robots based on the local concentration gradients. These methods are computationally lightweight and are often employed for use in swarm robotics [Marjovi and Marques, 2014, Wisnu et al., 2007] where resources are limited. However, they are heavily reliant on the presence of data and do not perform well in large scale scenarios or with sparse measurements.

The third class, and the method that is leveraged in the proposed system, is the information theoretic approach. Information theoretic approaches exploit the belief of the system state and try to take actions that reduce the uncertainty of a given estimate. Given this property, information theoretic approaches are inherently coupled to the estimation process and require some form of metric to quantify uncertainty. Within source term estimation, both Infotaxis [Vergassola et al., 2007] and Entrotaxis [Hutchinson et al., 2018] have been successfully employed for sparse search tasks. Infotaxis is concerned with reducing entropy based on the expectation of the posterior distribution, whereas Entrotaxis considers the entropy reduction based on the predictive measurement distribution. In a comparison between bio-inspired searches and information theoretic searches [Voges et al., 2014], the information theoretic solution is found to be more effective in problems which exhibit sparse data, thus performs well in real-world experiments [Hutchinson et al., 2019b,c]. Sparse measuring conditions are more conducive towards urban environments since complex geometry can obscure the plume from much of the search domain.

The information theoretic approach has also been seen in other applications. For example, Schmid et al. [2020] developed a sampling based path planner using RRT to evaluate the utility of sampling the environment at a specified location along a trajectory. This method allowed a sampling agent the ability to determine efficient sampling locations whilst navigating in complex environments, inherently coupling these two aspects. However, the nature of the work Schmid et al. [2020] is to explore the unknown environment, rather than locating the release source.

It is noted that the vast majority of research items that focus on the motion planning aspect of source search do so in an open environment and therefore this gap between open and urban scenarios is the key motivation for the research presented.

2.3 Source search in complex environments

Path planning in complex environments for source search has some studies but many do so in a heavily constrained environments and therefore are not optimised for the challenges of real urban scenarios. In Marjovi and Marques [2011], multi robot mapping and source localisation is performed using an anemotaxis approach wherein simultaneous localisation and mapping (SLAM) is performed until a threshold concentration is found, upon which the robot switches to a anemotaxis search. As with all gradient-based approaches, this system requires an increasing number of agents to cope with large scale situations. With the informed tree search algorithm we seek to address the scaling problem with adaptive sampling of the environment so that the system is broadly independent of the scale. This also means that a multi agent approach is not required to attain positive results. However, it is appreciated that multi agent approaches are generally more time efficient than their single agent counterpart (at the expense of increased resources).

In Zhao et al. [2020], the Entrotaxis-jump algorithm is proposed for source search in a large-scale road network. Entrotaxis-jump combines Entrotaxis with an intermittent search strategy that allows a myopic agent to traverse around obstacles if the utility of sampling in the direction of the obstacle is high. Whilst this method successfully increases the performance of Entrotaxis in urban environments, it assumes a simple Gaussian-like dispersion model adequately reflects the dispersion characteristics of a source release in a dense urban environment. Moreover, the trajectory generation is not explored in the search process and therefore for more complex geometries (i.e. not a road network), it is unknown if this method will be able to successfully navigate towards a source. Nevertheless, based on the findings of Zhao et al. [2020] it is clear that there is a benefit to intelligent goal selection methods compared to those in classical source search motion planning.

By employing the more advanced path planning techniques that have been adopted in other environmental monitoring fields and customising these methods to suit the challenges of the source search problem, we aim to bring a new level of operational efficiency and robustness to the field of CBRN related robotics.

3 Problem statement

The source search problem is formulated under the IPP framework in this Section.

Let $\mathbf{X} \subset \mathbb{R}^2$ be the state space of the search and planning problem, $\mathbf{X}_{\text{obs}} \subset \mathbf{X}$ be the states in collision with obstacles. Thus, the set of admissible states can be expressed as $\mathbf{X}_{\text{free}} := \mathbf{X} \setminus \mathbf{X}_{\text{obs}}$. Let $\mathbf{s} \in \mathbf{X}$ be the source location, $\mathbf{x}_k \in \mathbf{X}_{\text{free}}$ be the robot position at sampling instant k and $\mathbf{X}_{\text{goal}} \subset \mathbf{X}_{\text{free}}$ be the set of goal region. A collision-free path is continuous mapping $\sigma : \mathbb{R} \rightarrow \mathbf{X}_{\text{free}}$. Specifically, we define $\sigma_i^j(s)$, $s \in [0, 1]$, a path from $\sigma_i^j(0) = \mathbf{x}_i$ to $\sigma_i^j(1) = \mathbf{x}_j$. The traversal length of the path is denoted as $c(\sigma_i^j)$.

The problem considered in this work is to guide the robots to explore the free space to find the source location \mathbf{s} and eventually navigate to the goal region inclusive of the source location, such that $\mathbf{x}_k \in \mathbf{X}_{\text{goal}}(\mathbf{s})$. However, directly finding an optimal path or feasible path from initial position \mathbf{x}_{init} to \mathbf{s} is not possible, since the source location is unknown to the robot. In this case, a recursive IPP framework will be structured to address this problem.

Problem 1 (source term estimation) *At each sampling time k , the robot takes a measurement of the local chemical concentration $z_k(\mathbf{x}_k)$, which in conjunction with historical readings $\mathcal{Z}_k = \{z_k(\mathbf{x}_k), \mathcal{Z}_{k-1}\}$, can be used to estimate the source term Θ , in the form of its posterior distribution, i.e., $p(\Theta|\mathcal{Z}_k)$.*

Note that the source term Θ normally consists of source location \mathbf{s} , release rate Q and other relevant parameters that can be used to characterise a airborne release (see Hutchinson et al. [2019b] for more details). To facilitate the discussion we use $\theta_x^{(k)}$ to denote the estimated source location at sampling instant k .

Problem 2 (IPP) *Let σ_k^{k+1} be a collision-free path that can be executed by the robot, starting from the robot's current location \mathbf{x}_k to an end location \mathbf{x}_{k+1} . Let Σ be the set of such non-trivial paths to be constructed. The IPP problem is then formally defined as the search for a path, $\sigma^* \in \Sigma$, that minimise a utility function $\Psi(\cdot)$, such that*

$$\sigma^* := \arg \min_{\sigma \in \Sigma} \{\Psi(\sigma) | \sigma(0) = \mathbf{x}_k, c(\sigma) \leq \bar{c}\} \quad (1)$$

where \bar{c} is the upper bound of the path length.

Note that the objective of the path planning problem is to find the most informative sampling location at the end of the path σ^* . This is because the chemical sensing robot normally takes point measurements to accommodate the response time of the chemical sensor.

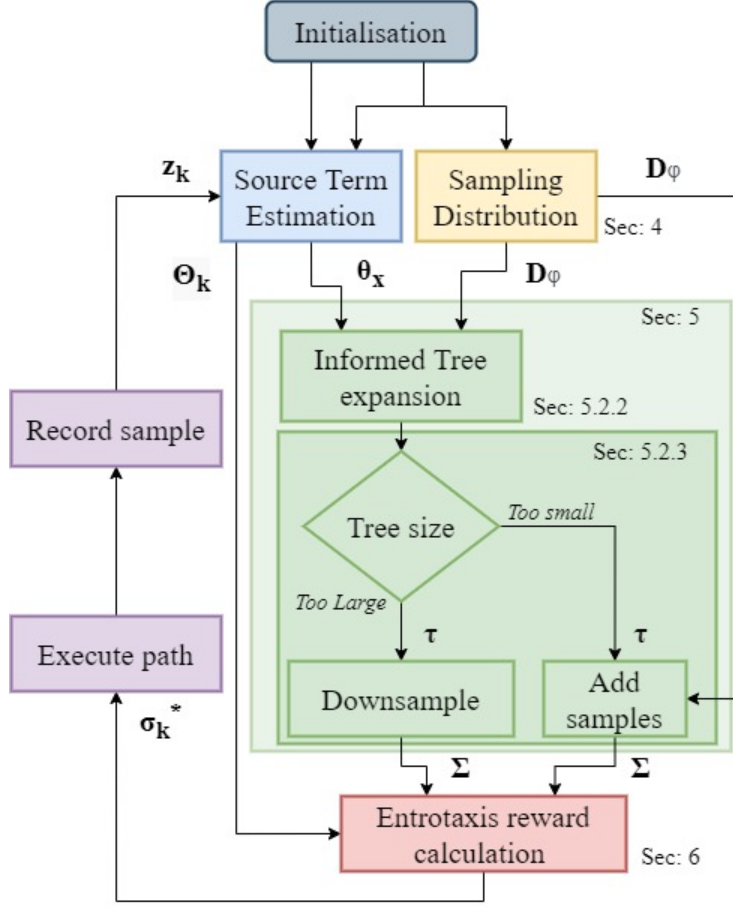


Figure 1: Architecture of the proposed source search algorithm

The proposed framework is to recursively solve Problem 1 and 2 such that the robot can be guided to the source region $\mathbf{X}_{\text{goal}}(\mathbf{s})$. At each sampling instant k , the robot takes the sensor reading z_k to update the source term estimation $p(\Theta|Z_k)$. Such a posterior distribution can be used to inform the design of the set Σ , so that Problem 2 can be constructed and subsequently solved to generate the next sampling location at the end of σ_k^* .

In this work, Problem 1 is solved by using an established particle filter developed in Hutchinson et al. [2019b], so its implementation detail is skipped for the sake of brevity. The key challenge that remains open is how to efficiently construct the set of candidate paths Σ in Problem 2, which should 1) reduce the chance of taking samples downwind of buildings, 2) guarantee collision-free control actions and 3) strike a good balance between exploitation and exploration. To end this, an informed tree search algorithm is developed and integrated into the proposed framework as outlined in Fig. 1. Each part of the downward running system will be explained in further detail in the order that they are performed during one iteration of the planning loop.

4 Generation of sampling locations

Many STE algorithms for predicting the source parameter distribution (e.g. Ristic et al. [2016], Hutchinson et al. [2018], Zhao et al. [2020]), whilst proven in ideal open environments, have drawbacks when used in a feature rich environments. Because obstacle interactions with the gas dispersion are not accounted for (and the use of such a computationally expensive model is unsuitable for mobile robotics), the intelligent use of how sample locations are chosen can be leveraged to mitigate the incongruity of the model and the physical system.

As defined in the problem statement, the set of admissible states that are considered for the search and planning problem is defined as \mathbf{X}_{free} . When using a sampling based path planner, traditionally a single sample state \mathbf{x}_m is drawn such that $\mathbf{x}_m \leftarrow \{\mathbf{D} \sim \mathbf{U}(\mathbf{X}_{\text{free}})\}$, where \mathbf{D} represents the uniform distribution of states that exist within free space. We

also define the notation $\mathbf{X}_m \leftarrow \{\mathbf{D} \sim \mathbf{U}(\mathbf{X}_{\text{free}})\}_{1:N}$, where \mathbf{X}_m is a set of samples with size N , uniformly drawn from free space.

In traversability planning, the definition of \mathbf{X}_{free} is adequate for dictating how sample states should be drawn and therefore a uniform distribution is most often used. However, as stated in [Karaman and Frazzoli, 2011], the sampling framework can extend to any distribution with a density bounded away from 0 upon \mathbf{X}_{free} . In source term estimation, it is intuitive that the robot should sample in areas where it is most likely to interact with the target source, which is not uniform over the free space.

Obstacle interactions with scalar wind fields lead to complex flow dynamics that take significant resources to resolve. However, it can be said that for a particle that exists in a wind field, the most likely trajectory of the particle will be in the wind direction ϕ , and that obstacles will create isolated areas behind the obstacle that blocks flow. It is in these areas that is less likely for a robot to interact with the source plume and therefore a sample distribution \mathbf{D}_ϕ should be attained that stipulates the robot should sample less in these areas.

\mathbf{D}_ϕ is derived (similarly to [Bellingham et al., 2002]) by calculating the divergent effect that an obstacle would have on a particle entering the search space using Dijkstra’s search (detailed below and shown in Fig. 2). The sample generation technique can be expensive to calculate for large maps and therefore should be performed at a reasonable resolution. Samples can be drawn repeatedly from the same distribution assuming the conditions that the wind direction ϕ does not change significantly and that the obstacle map is static. The sample generation methodology comprises one of the main new contributions to the field of source search and feeds directly into the second new contribution, the informed tree search.

4.1 Sample distribution algorithm

To generate a probability distribution that reflects the obstacle interactions with the wind field, firstly a set of starting states that represents the inlet of a particulate to the search space \mathbf{X} is defined as $\mathbf{X}_{\text{inlet}}$ (red line in Fig. 2). These inlet states are akin to the inlet condition of a CFD model thus the location of these states is dependent on the wind field direction ϕ , which can be initiated with the prior of θ_ϕ from the Bayesian inference. Dijkstra’s search is then performed on the discrete state obstacle map (e.g. an occupancy grid) using $\mathbf{X}_{\text{inlet}}$ as starting conditions. The vertices of the Dijkstra network \mathbf{V}_{obs} are defined as all $\mathbf{x} \in \mathbf{X}_{\text{free}}$ and edges of traversal \mathbf{E}_{obs} lie between obstacle free adjacent vertices. This then generates the average cost \mathbf{C}_{obs} of getting from all $\mathbf{x} \in \mathbf{X}_{\text{inlet}}$ to all $\mathbf{x} \in \mathbf{X}_{\text{free}}$. A second cost map is also calculated using Dijkstra’s search on the obstacle free map using $\mathbf{X}_{\text{inlet}}$. The vertices of the second network \mathbf{V}_{open} are defined as all $\mathbf{x} \in \mathbf{X}$ and edges of traversal \mathbf{E}_{open} lie between any adjacent vertices. This second cost map represents how an inlet particle would traverse the domain uninterrupted by the obstacles. \mathbf{C}_{open} is then subtracted from \mathbf{C}_{obs} leaving a final cost map \mathbf{C}_ϕ that represents how the obstacles have negatively interrupted the wind field. \mathbf{C}_ϕ can then be used to give the probability distribution \mathbf{D}_ϕ , by adding the minimum value of \mathbf{C}_ϕ . \mathbf{D}_ϕ is now bound away from 0 upon \mathbf{X}_{free} and can be used to draw samples from which to grow the informed tree. This process is summarised in Algorithm 1.

5 IPP Informed tree search

The second main contribution of the paper is the informed tree procedure, which acquires a set of obstacle free trajectories that help the robot achieve its goal of localising an unknown source within a feature rich search space. The informed tree search procedure can be separated into two distinct parts: tree expansion and path selection. Tree expansion is concerned with finding admissible paths to the goal location whereas path selection decides the set of paths to be evaluated by the utility function. Both parts are described below and further detail is given in section 5.2.

To establish possible gas sampling locations and an initial set of admissible paths, an RGG is defined which contains a set of sampled states, $\mathbf{G} \in \mathbf{X}_{\text{free}}$ (Fig 3a, 4a). Samples are drawn in weighted free space, of sample size N , with the weighting on samples derived from the likely gas particle path distribution \mathbf{D}_ϕ described in Section 4. The parameter N is chosen such that the informed tree search can fully explore the area \mathbf{X}_{free} . The base of the tree is set to \mathbf{x}_k , and the goal set is defined as the k_n -nearest $\mathbf{x} \in \mathbf{G}$ to the best estimate of the source location (other definitions of goal sets are also applicable). For the rest of the paper, $\mathbb{E}(\mathbf{s})$ is used as the best estimate.

The tree is then heuristically constructed towards the goal set, in a similar manner to [Gammell et al., 2015], until a valid path is found (Fig 3b, 4b). However unlike [Gammell et al., 2015], after one batch search has been completed, another batch is not initiated. This is because we are not trying to acquire the shortest trajectory towards the estimated source location. Instead, we need only a set of admissible and exploratory paths to the source that can guide the search in a way that will converge on the source location.

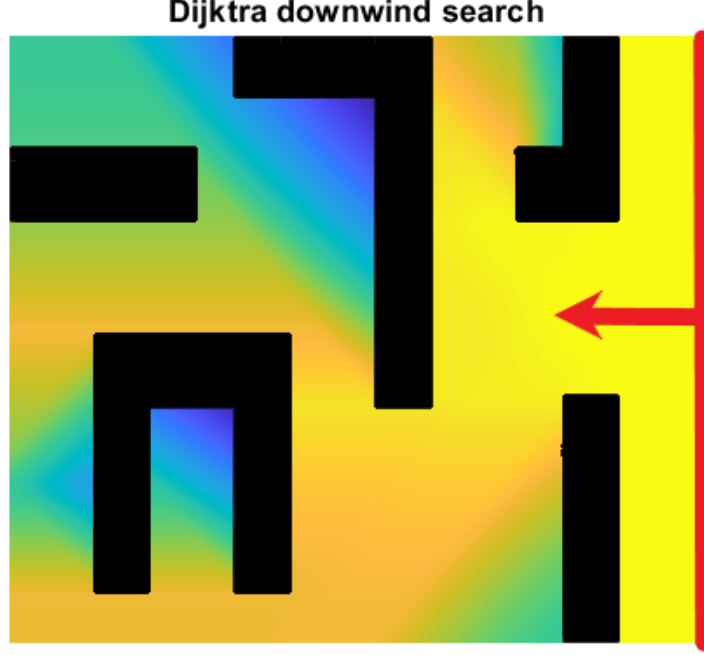


Figure 2: Sample distribution of the likely trajectory of an inlet gas particle, attained from Dijkstra’s search on an occupancy grid. Yellow indicates a high likelihood whilst blue indicates a low likelihood. Red arrow shows the wind direction.

Algorithm 1: Sample Generation ($\mathbf{X}, \mathbf{X}_{inlet}$)

```

1 Procedure init()
2    $\mathbf{V}_{obs} \leftarrow \mathbf{x} \in \mathbf{X}_{free}$ 
3    $\mathbf{C}_{obs} \leftarrow \sum \text{Dijkstra}(\mathbf{V}_{obs}, \mathbf{E}_{obs}, \forall \mathbf{x} \in \mathbf{X}_{inlet})$ 
4    $\mathbf{V}_{open} \leftarrow \mathbf{x} \in \mathbf{X}$ 
5    $\mathbf{C}_{open} \leftarrow \sum \text{Dijkstra}(\mathbf{V}_{open}, \mathbf{E}_{open}, \forall \mathbf{x} \in \mathbf{X}_{inlet})$ 
6    $\mathbf{C}_{\phi} \leftarrow \mathbf{C}_{open} - \mathbf{C}_{obs}$ 
7    $\mathbf{D}_{\phi} \leftarrow \mathbf{C}_{\phi} + \arg \min_{\mathbf{x} \in \mathbf{X}_{free}} \mathbf{C}_{\phi}(\mathbf{x})$ 
8 Procedure sample(N)
9    $\mathbf{X}_m \leftarrow \{\mathbf{D}_{\phi}(\mathbf{X}_{free})\}_{1:N}$ 
10  return  $\mathbf{X}_m$ 

```

Once a path to the goal set is found, the tree is pruned (Fig 3c, 4c), and then must be either upsampled or down-sampled in order to match the computational requirements of the IPP. This is driven by the desired number of paths $|\Sigma|$, to be calculated in (1). If the tree contains paths $\geq |\Sigma|$, then the pruned tree is downsampled, as shown in Fig 3d, to the first $|\Sigma|$ paths stemming from \mathbf{x}_k . If more samples are required, then the tree is expanded by taking further samples (again from weighted free space) that extend the tree as shown in Fig 4d. This expansion is bound within an ellipse that accounts for the uncertainty of the source estimate in θ_x (derived in section 5.2.3). Once the path set Σ has been established, the set is passed for utility calculation. The detailed derivation of informed tree search is provided in this section.

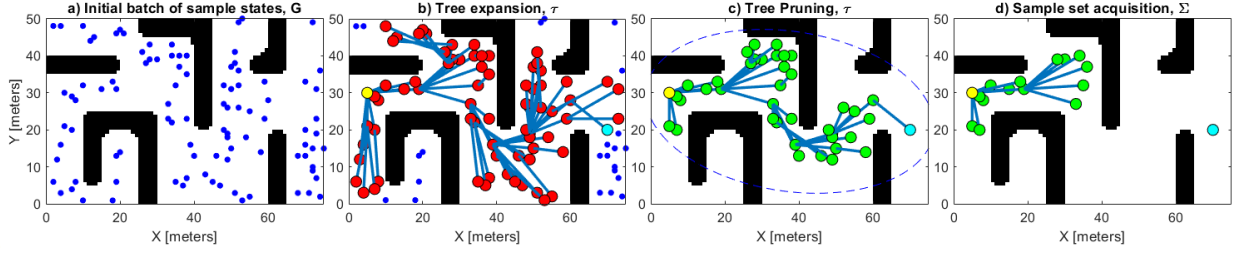


Figure 3: Informed tree search with a starting location $\mathbf{x}_k = [5, 30]$ (yellow circle) and goal location $\mathbf{x}_{goal} = [70, 20]$ (cyan circle). a) The initial batch of sample states $\mathbf{x} \in \mathbf{G}$ (blue dots) drawn from the discrete probability distribution \mathbf{D}_ϕ where $N = 100$ and θ_ϕ is in the negative x -direction. b) Tree expansion procedure until the goal found, tree vertices $\mathbf{v} \in \mathbf{V}$ shown with red circles and tree edges $(\mathbf{v}, \mathbf{w}) \in \mathbf{E}$ shown with blue lines. c) Tree pruning with remaining vertices with green circles and the ellipse that represents the pruning criterion shown with a blue dashed line. d) Downsampling of the pruned tree to contain the first $|\Sigma| = 15$ vertices in the tree.

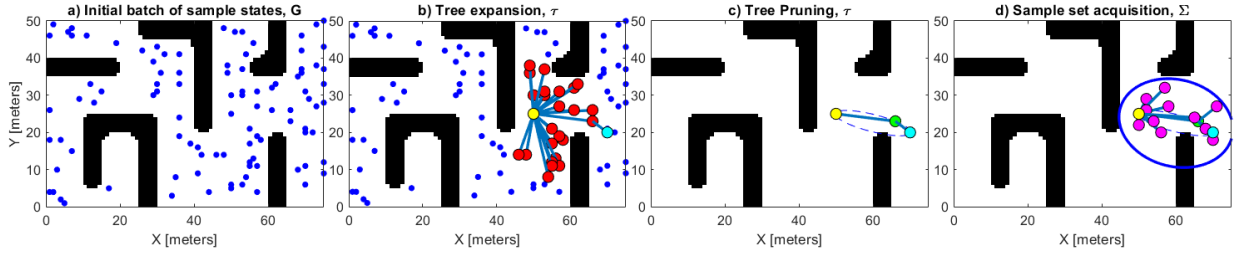


Figure 4: Informed tree search with a starting location $\mathbf{x}_k [50,25]$ (yellow circle) and goal location $\mathbf{x}_{goal} [70,20]$ (cyan circle). a) The initial batch of sample states $\mathbf{x} \in \mathbf{G}$ (blue dots) drawn from the discrete probability distribution \mathbf{D}_ϕ where $N = 100$ and θ_ϕ is in the negative x -direction. b) Tree expansion procedure until the goal found, tree vertices $\mathbf{v} \in \mathbf{V}$ shown with red circles and tree edges $(\mathbf{v}, \mathbf{w}) \in \mathbf{E}$ shown with blue lines. c) Tree pruning with remaining vertices with green circles and the ellipse that represents the pruning criterion shown with a blue dashed line. d) Adding of further samples within the expanded ellipse (dark blue solid line) given a source position uncertainty $\sigma_{\theta_x} = 5m$. New samples added are shown with magenta circles.

5.1 Notation

To facilitate the derivation of the informed tree search algorithm, some notations are defined in this sub-section. The function $\hat{\mathbf{g}}(\mathbf{x})$ relates to the estimated cost to come from the start (i.e., \mathbf{x}_k) to a state $\mathbf{x} \in \mathbf{G}$, and $\hat{\mathbf{h}}(\mathbf{x})$ is the estimated cost to go from the state to the goal set \mathbf{X}_{goal} . These functions can be evaluated using the Euclidean distance between two states. Then, $\hat{\mathbf{f}}(\mathbf{x})$ is the estimated cost from the start \mathbf{x}_k , to the goal set, given the path passes through \mathbf{x} , i.e. $\hat{\mathbf{f}}(\mathbf{x}) := \hat{\mathbf{g}}(\mathbf{x}) + \hat{\mathbf{h}}(\mathbf{x})$. If the current best solution to the goal set is defined as \mathbf{c}_{best} , then this function can define a subset of states that potentially give a better solution to the goal i.e. $\mathbf{X}_{\hat{\mathbf{f}}} := \{\mathbf{x} \in \mathbf{G} | \hat{\mathbf{f}}(\mathbf{x}) \leq \mathbf{c}_{best}\}$.

The tree with vertices $\mathbf{V} \subseteq \mathbf{G}$ and edges $\mathbf{E} = (\mathbf{v}, \mathbf{w})$ for vertices $\mathbf{v} \in \mathbf{V}$ and $\mathbf{w} \in \mathbf{V}$, is defined as $\mathcal{T} := (\mathbf{V}, \mathbf{E})$. From the current tree, the cost to come to a state $\mathbf{x} \in \mathbf{G}$ is given by the function $\mathbf{g}_\tau(\mathbf{x})$. Any state that is not in the tree is assumed to have a cost ∞ . If the optimal cost to come to a state is defined as $\mathbf{g}(\mathbf{x})$, then it is seen that, $\forall \mathbf{x} \in \mathbf{G}, \hat{\mathbf{g}}(\mathbf{x}) \leq \mathbf{g}(\mathbf{x}) \leq \mathbf{g}_\tau(\mathbf{x})$.

The cost of an edge between states $\mathbf{x}, \mathbf{y} \in \mathbf{G}$ and the estimated cost of said edge are defined as $\mathbf{c}(\mathbf{x}, \mathbf{y})$ and $\hat{\mathbf{c}}(\mathbf{x}, \mathbf{y})$. Any edge that intersects an obstacle is assumed to have an infinite cost thus defining that $\forall \mathbf{x}, \mathbf{y} \in \mathbf{G}, \hat{\mathbf{c}}(\mathbf{x}, \mathbf{y}) \leq \mathbf{c}(\mathbf{x}, \mathbf{y}) \leq \infty$. Calculating $\mathbf{c}(\cdot)$ is computationally expensive due to the need to account for obstacle collisions and dynamic constraints and therefore the heuristic estimate $\hat{\mathbf{c}}(\cdot)$ is used to delay calculating this where possible. In the scenario where there are no dynamic constraints on the system, then an obstacle free edge $\hat{\mathbf{c}}(\cdot) = \mathbf{c}(\cdot)$.

The Lebesgue measure of a set is written as, $\lambda(\cdot)$, and the Lebesgue measure of an n -dimensional unit ball, is ζ_n . $|\cdot|$ refers to the cardinality of a set. $X \stackrel{\pm}{\leftarrow} \{x\}$ and $X \stackrel{-}{\leftarrow} \{x\}$ are shorthand notation for $X = X \cup \{x\}$ and $X = X \setminus \{x\}$ respectively.

Algorithm 2: Informed tree expansion ($N, \mathbf{x}_k, \theta_x^{(k)}$)

```

1  $\mathbf{G} \leftarrow \text{sample}(N)$ 
2  $\mathbf{x}_{goal} \leftarrow \mathbb{E}(\theta_x^{(k)})$ 
3  $\mathbf{X}_{goal} \leftarrow \{ \arg \min_{\mathbf{X} \subseteq \mathbf{G}} \|\mathbf{x}_{goal} - \mathbf{X}\|_2 \mid |\mathbf{X}| = k_n \}$ 
4  $\mathbf{V} \leftarrow \mathbf{x}_k$ ;  $\mathbf{E} \leftarrow \emptyset$ ;  $\mathbf{Q}_e \leftarrow \emptyset$ ;  $\mathbf{Q}_v \leftarrow \mathbf{V}$ 
5  $r \leftarrow 2\kappa(1 + \frac{1}{n})^{\frac{1}{n}} (\frac{\lambda(X_{\hat{f}})}{\zeta_n})^{\frac{1}{n}} (\frac{\log(|\mathbf{G}|)}{|\mathbf{G}|})^{\frac{1}{n}}$ 
6 while  $\mathbf{Q}_v \neq \emptyset$  &  $g_\tau(\mathbf{x}) \in \mathbf{X}_{goal} = \infty$  do
7    $\mathbf{v}_m \leftarrow \arg \min_{\mathbf{x} \in \mathbf{Q}_v} \hat{\mathbf{f}}(\mathbf{x})$ 
8    $\mathbf{Q}_v \leftarrow \bar{\mathbf{v}}_m$ 
9    $\mathbf{V}_{near} \leftarrow \{ \mathbf{w} \in \mathbf{G} \mid \|\mathbf{v}_m - \mathbf{w}\|_2 \leq r \}$ 
10   $\mathbf{Q}_e \leftarrow \bar{\mathbf{v}}_m \cup \{ (\mathbf{v}_m, \mathbf{w}) \in \mathbf{V}_{near} \}$ 
11  while  $\mathbf{Q}_e \neq \emptyset$  do
12     $\mathbf{w}_m \leftarrow \arg \min_{\mathbf{w} \in \mathbf{Q}_e} \hat{\mathbf{c}}(\mathbf{v}_m, \mathbf{w}) + \hat{\mathbf{h}}(\mathbf{w})$ 
13     $\mathbf{Q}_e \leftarrow \bar{(\mathbf{v}_m, \mathbf{w}_m)}$ 
14    if  $g_\tau(\mathbf{v}_m) + \mathbf{c}(\mathbf{v}_m, \mathbf{w}_m) < g_\tau(\mathbf{w}_m)$  then
15      if  $\mathbf{w}_m \in \mathbf{V}$  then
16         $\mathbf{E} \leftarrow \bar{\mathbf{v}}_m \cup \{ (\mathbf{v}, \mathbf{w}_m) \in \mathbf{E} \}$ 
17      else
18         $\mathbf{V} \leftarrow \bar{\mathbf{w}}_m$ 
19         $\mathbf{Q}_v \leftarrow \bar{\mathbf{w}}_m$ 
20      end
21       $\mathbf{E} \leftarrow \bar{(\mathbf{v}_m, \mathbf{w}_m)}$ 
22    end
23  end
24 end
25 return  $\mathcal{T}(\mathbf{V}, \mathbf{E})$ 

```

5.2 Informed tree algorithms

Algorithm 2 outlines the tree expansion procedure during a single query event given the sampled states \mathbf{G} , the robots current location \mathbf{x}_k , and the current PDF of the source location $\theta_x^{(k)}$.

5.2.1 Initialisation (Alg 2, Lines 1:5)

To initialise, the goal state \mathbf{x}_{goal} is defined as $\mathbb{E}(\theta_x^{(k)})$, from which the goal set \mathbf{X}_{goal} is defined as the k_n nearest $\mathbf{x} \in \mathbf{G}$. The tree vertices set \mathbf{V} is set to \mathbf{x}_k , the tree edges \mathbf{E} and edge queue \mathbf{Q}_e are set to empty, and the vertex queue \mathbf{Q}_v , is set to \mathbf{V} . The edge queues exist to track which vertex and edge should be processed for adding to the tree. The radius r can also be defined during initialisation since only a single batch is being performed. The radius is calculated using the scaling parameter κ , the problem dimensionality n and the number of sampled states $|\mathbf{G}|$, as described in [Gammell et al., 2015].

5.2.2 Tree expansion (Alg 2, Lines 5:25)

The tree is expanded until \mathbf{Q}_v is empty (i.e. all $\mathbf{x} \in \mathbf{G}$ have been checked), or one of the states $\mathbf{x} \in \mathbf{X}_{goal}$ have a valid path in the tree. To determine which node should be selected for expansion, \mathbf{v}_m , the state $\mathbf{x} \in \mathbf{Q}_v$ with the lowest

Algorithm 3: Sample set acquisition ($\mathcal{T}(\mathbf{V}, \mathbf{E})$)

```

1  $\mathbf{V} \leftarrow \{ \mathbf{v} \in \mathbf{V} \mid \widehat{\mathbf{f}}(\mathbf{v}) > \mathbf{c}_{best} \}$ 
2  $\mathbf{E} \leftarrow \{ (\mathbf{v}, \mathbf{w}) \in \mathbf{E} \mid \widehat{\mathbf{f}}(\mathbf{v}) > \mathbf{c}_{best} \text{ or } \widehat{\mathbf{f}}(\mathbf{w}) > \mathbf{c}_{best} \}$ 
3 if  $|\mathbf{V}| > |\Sigma|$  then
4    $r \leftarrow 2\kappa \left(1 + \frac{1}{n}\right)^{\frac{1}{n}} \left(\frac{\lambda(X\hat{f})}{\zeta_n}\right)^{\frac{1}{n}} \left(\frac{\log(|\mathbf{V}|)}{|\mathbf{V}|}\right)^{\frac{1}{n}}$ 
5   while  $|\mathbf{V}| < |\Sigma|$  do
6      $\mathbf{x}_m \leftarrow \text{sample}(1) \mid \widehat{\mathbf{f}}(\mathbf{x}_m) \leq \mathbf{c}_{best} + 2\sigma_{\theta_x^{(k)}}$ 
7      $\mathbf{V}_{near} \leftarrow \{ \mathbf{v} \in \mathbf{V} \mid \|\mathbf{x}_m - \mathbf{v}\|_2 \leq r \}$ 
8      $\mathbf{Q}_e \leftarrow \{ (\mathbf{v}, \mathbf{x}_m) \in \mathbf{V}_{near} \}$ 
9     while  $\mathbf{Q}_e \neq \emptyset$  do
10       $\mathbf{v}_m \leftarrow \arg \min_{\mathbf{v} \in \mathbf{Q}_e} \|\mathbf{x}_m - \mathbf{v}\|_2$ 
11       $\mathbf{Q}_e \leftarrow (\mathbf{v}_m, \mathbf{x}_m)$ 
12      if  $\mathbf{g}_\tau(\mathbf{v}_m) + \mathbf{c}(\mathbf{x}_m, \mathbf{v}_m) < \mathbf{g}_\tau(\mathbf{x}_m)$  then
13        if  $\mathbf{x}_m \in \mathbf{V}$  then
14           $\mathbf{E} \leftarrow \{ (\mathbf{v}, \mathbf{x}_m) \in \mathbf{E} \}$ 
15        else
16           $\mathbf{V} \leftarrow \mathbf{x}_m$ 
17        end
18         $\mathbf{E} \leftarrow (\mathbf{v}_m, \mathbf{x}_m)$ 
19      end
20    end
21  end
22 else
23    $\mathbf{V}_m \leftarrow \{ \arg \min_{\mathbf{V}_m \subseteq \mathbf{V}} \mathbf{g}(\mathbf{V}_m) \mid |\mathbf{V}_m| = |\Sigma| \}$ 
24    $\mathbf{V} \leftarrow \mathbf{V}_m$ 
25    $\mathbf{E} \leftarrow \{ (\mathbf{v}, \mathbf{w}) \in \mathbf{E} \mid \mathbf{v} \notin \mathbf{V} \text{ or } \mathbf{w} \notin \mathbf{V} \}$ 
26 end
27 return  $\mathcal{T}(\mathbf{V}, \mathbf{E})$ 

```

estimated cost from the start to the goal, $\widehat{\mathbf{f}}(\mathbf{x})$, is selected for expansion. The set \mathbf{V}_{near} is defined around the expansion node which contains all states \mathbf{w} in \mathbf{G} that are within the radius r of \mathbf{v}_m . The edges that connect all \mathbf{w} to \mathbf{v}_m are then added to the queue \mathbf{Q}_e .

Once the edge queue \mathbf{Q}_e has been defined, each edge is processed by selecting the $\mathbf{w} \in \mathbf{Q}_e$ with the lowest estimated cost from the expanded vertex \mathbf{v}_m to the goal, that passes through \mathbf{w} (Alg 2, Line 13). The chosen edge is then removed from \mathbf{Q}_e . The edge will be added to the tree subject to the condition in Alg 2, Line 15. This is that the actual cost (including collisions) to \mathbf{w}_m via \mathbf{v}_m is less than the tree cost $\mathbf{g}_\tau(\mathbf{w}_m)$ (if \mathbf{w}_m is not already in the tree then this is guaranteed).

If \mathbf{w}_m is already in \mathbf{V} , then its existing edge $(\mathbf{v}, \mathbf{w}_m)$ is removed from \mathbf{E} and the new edge $(\mathbf{v}_m, \mathbf{w}_m)$ is added. If \mathbf{w}_m is not in the tree then it is added to \mathbf{V} and also to the vertex queue \mathbf{Q}_v (for future vertex expansion). The vertex expansion process is then ended when all edges of \mathbf{v}_m have been checked i.e. \mathbf{Q}_e is empty. When all vertices have been expanded or a path to the goal has been found, then the tree $\mathcal{T}(\mathbf{V}, \mathbf{E})$ is returned for candidate selection.

5.2.3 Sample set acquisition (Alg 3)

The full tree \mathcal{T} from the initial search is groomed in Alg 3 in order to meet computational requirements of the IPP. Firstly, the tree is pruned so that only vertices in \mathbf{V} and edges in \mathbf{E} which can possibly improve (or are part of) the current solution are kept for consideration (Alg 3, Lines 1:2). In the case where no solution is found, i.e. $c_{best} = \infty$, then \mathbf{V} and \mathbf{E} remain unchanged.

After pruning, tree blossoming or tree culling will occur. The tree will be further expanded (blossoming) if there are not enough vertices in \mathbf{V} to match $|\Sigma|$ (Alg 3, Lines 4:21), or further reduced (culling) if there are more vertices in \mathbf{V} than can be efficiently computed for their utility (Alg 3, Line 23:25)

For a given tree \mathcal{T} where $|\mathbf{V}| < |\Sigma|$, the tree is expanded with a new search radius r defined by the current state of the tree (Alg 3, Line 4). To give more potential sampling locations from which to evaluate utility, a new query state \mathbf{x}_m is sampled from weighted free space $\mathbf{x} \in \mathbf{X}_{free} \mid \mathbf{D}_\phi$ subject to the constraint that $\hat{\mathbf{f}}(\mathbf{x}) \leq c_{best} + 2\sigma_{\theta_x^{(k)}}$ (Alg 3, Line 6). The addition of including source location uncertainty is necessary in order to account for the fact that it is probabilistically likely that the true \mathbf{x}_s lies within 2 standard deviations of the goal \mathbf{x}_{goal} and therefore new exploratory samples should be drawn accounting for this. Furthermore, as $c_{best} \rightarrow 0$, $\mathbf{x} \in \mathbf{X}_{free} \rightarrow \emptyset$ and therefore to avoid this local minimum, the robot should attempt to search in an area relative to the uncertainty of its estimate. Alg 3, Lines 7:20 follows closely to the tree expansion process of Alg 2, Lines 11:23. The difference being that we are now attempting to connect the unconnected state \mathbf{x}_m to one of the vertices in the tree (as opposed to expanding the tree into the unconnected set). If a sampled state \mathbf{x}_m cannot be connected to the tree, then the criterion at Alg 3, Line 12 will always fail and a new state will be initiated with \mathbf{V} and \mathbf{E} remaining unchanged. Once the number of vertices in the tree equals $|\Sigma|$, then the final state of \mathcal{T} is returned for utility calculation. This expansion process is similar in formulation to Alg 2 however single query states are attached to the tree set as opposed to the tree expanding into the unconnected set.

If for a given tree \mathcal{T} , where $|\mathbf{V}| \geq |\Sigma|$, the tree is culled as per Alg 3, Lines 23:25. A query set of vertices \mathbf{V}_m is defined which takes the first $|\Sigma|$ number of $\mathbf{v} \in \mathbf{V}$ which have the lowest tree cost. Since \mathbf{V} has already been pruned, the remaining branches in \mathbf{V}_m are towards the goal whilst allowing for some exploratory states around the path to the goal. \mathbf{V} is then updated to the new set \mathbf{V}_m and any edges that contain old vertices are removed from \mathbf{E} (Alg 3, Line 25). Given the scenario where $c_{best} = \infty$, then \mathbf{V}_m will be a non-directional set of nodes that were connected to \mathbf{x}_k during tree expansion.

6 IPP Utility calculation

Given the robot has acquired a set candidate trajectories Σ , the robot needs to select the trajectory and the sample location that will minimise Eq. (1). Several definitions of the utility function $\Psi(\cdot)$ can be used together with parametric modelling techniques such as the Bayesian inference used here. Based on the results attained in [Hutchinson et al., 2018], the Entrotaxis measure of information gain has proven to be effective in source search and therefore is the chosen metric when defining the utility function. Entrotaxis attempts to find the most informative location by considering the entropy of the predictive measurement distribution at a sample location, therefore, we define this location as $\sigma(1)$ given the start of the trajectory $\sigma(0)$. In Entrotaxis, the Shannon Entropy $\mathbf{H}(\cdot)$ is used as the expected information measure as follows:

$$\Psi(\sigma) = - \int P(\hat{\mathbf{z}}_{k+1}(\sigma) | \mathbf{z}_{1:k}) \log P(\hat{\mathbf{z}}_{k+1}(\sigma) | \mathbf{z}_{1:k}) d\hat{\mathbf{z}}_{k+1} \quad (2)$$

where $\hat{\mathbf{z}}_{k+1}(\sigma)$ refers to the unknown measurement at the potential sampling position of $\sigma(1) \in \Sigma$. This unknown measurement will not be known until the location is physically sampled and therefore the probability of the expected number of particle encounters $P(\hat{\mathbf{z}}_{k+1}(\sigma) | \mathbf{z}_{1:k})$ is derived using the posterior distribution of the source Θ_k :

$$\begin{aligned} & P(\hat{\mathbf{z}}_{k+1}(\sigma) | \mathbf{z}_{1:k}) \\ &= \int_{\Theta_{k+1}} P(\hat{\mathbf{z}}_{k+1}(\sigma), \Theta_{k+1} | \mathbf{z}_{1:k}) d\Theta_{k+1} \\ &= \int_{\Theta_{k+1}} P(\hat{\mathbf{z}}_{k+1}(\sigma) | \Theta_{k+1}) P(\Theta_{k+1} | \mathbf{z}_{1:k}) d\Theta_{k+1} \\ &\approx \sum_{i=1}^n w_k^{(i)} \cdot P(\hat{\mathbf{z}}_{k+1}(\sigma) | \Theta_{k+1}^{(i)}) \end{aligned} \quad (3)$$

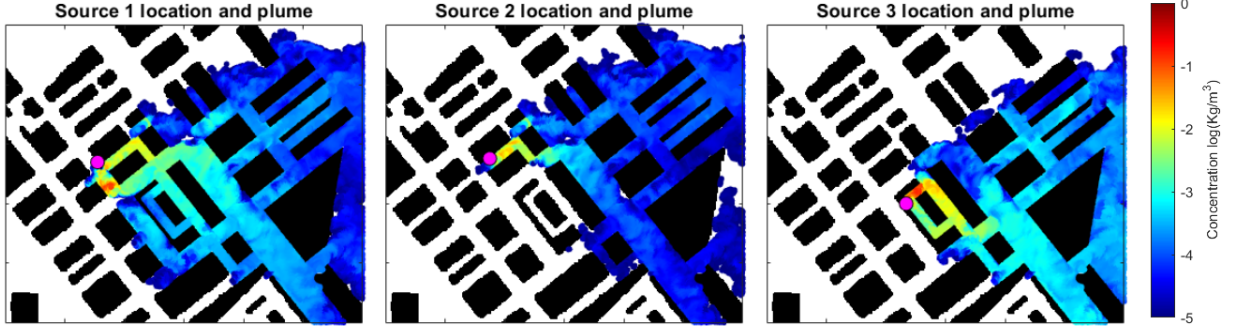


Figure 5: Snapshot concentration colour map for each of the 3 tested sources, superimposed onto the occupancy map (time= 0s). Concentrations are coloured as $\log(\text{Kg/m}^3)$ with concentrations below $10\mu\text{g/m}^3$ not coloured. Source location is shown as a magenta circle. Sources 1 & 3 are vented sources with a perturbation of 1m/s and source 2 is a passive source with no excitation.

where the weighted samples $\{\Theta_k^{(i)}, w_k^{(i)}\}_{i=1}^n$ constitutes the posterior distribution $P(\Theta_k|\mathbf{z}_{1:k})$ and $\Theta_{k+1}^{(i)} = \Theta_k^{(i)}$ [Hutchinson et al., 2019b]. To reduce computational load, a much smaller number of samples $\{\Theta_k^{(l)}, 1/n_z\}_{l=1}^{n_z}$ is resampled from the full posterior, where $n_z \ll n$, to give a possible future measurement set of $\{\hat{\mathbf{z}}_{k+1}^{(l)}\}_{l=1}^{n_z}$ and reduce Eq. (3) to:

$$P(\hat{\mathbf{z}}_{k+1}(\sigma)|\mathbf{z}_{1:k}) \approx \frac{1}{n_z} \sum_{l=1}^{n_z} \delta(\hat{\mathbf{z}}_{k+1} - \hat{\mathbf{z}}_{k+1}^{(l)}) \quad (4)$$

Substituting Eq. (4) into Eq. (2) allows the entropy for performing the trajectory $\Psi(\sigma)$, to be approximated by summing over the possible future measurements.

$$\Psi(\sigma) \approx \frac{1}{n_z} \sum_{l=1}^{n_z} \hat{w}_{k+1}^{(i,l)} \log \hat{w}_{k+1}^{(i,l)} \quad (5)$$

$\Psi(\cdot)$ is then calculated for all $\sigma \in \Sigma$ and minimised as per Eq. (1), to give the optimal trajectory σ_k^* . The Entrotaxis reward function is calculated every time a new set of Σ is defined from the informed tree search.

At this point in the system, the IPP has taken an informed set of potential trajectories from the informed tree search, performed predictive modelling on this subset of samples to calculate predicted information gain for each trajectory, and then chosen the optimal solution to be executed by a low-level path planner.

This defines a single control loop of the proposed source search system. The inference, informed tree search and utility calculation procedures are then repeated iteratively as per Fig. 1 until an end constraint on the system is met, e.g., a time budget.

7 Simulation

A set of simulation studies have been carried out to verify the proposed autonomous search algorithm in a large scale, outdoor, feature rich environment. The staging for the study is the DAPPLE dispersion experiment [Martin et al., 2010] and consists of a wind tunnel validated CFD simulation of a source release under steady wind conditions in urban London. This dataset contains a complex series of urban canyons which cause local wind field instabilities that not only tests the algorithms ability to predict the source from a single value wind field, but also the efficient path finding abilities of the main contribution of this paper, i.e., the informed tree search.

There are 3 source locations within the same DAPPLE domain that can be tested as shown in Fig. 5. Sources 1 & 3 are modelled as active vent releases of outlet velocity 1m/s whilst source 2 is a passive release where the main method of transportation is the local wind field formed inside the urban environment. At the initialisation of the each source i.e. $k = 0\text{s}$, the plume structure is quasi-stable and therefore is only locally fluctuating, whilst the main plume structures are stable. All sources are modelled as constant release, matching the assumption made in the estimation model.

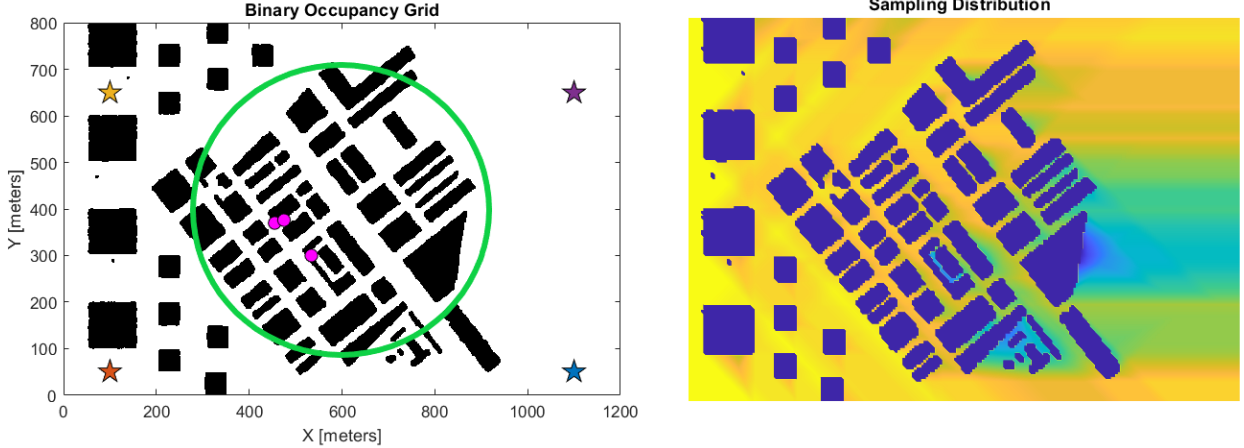


Figure 6: Left: $960,000\text{m}^2$ search area showing obstacles (black), starting positions 1, 2, 3 & 4 (blue, red, orange & purple stars), 3 source locations (magenta circles) and the initial prior source location area defined in $\theta_{x,y}$ (green circle). Right: Sample generation distribution attained from Dijkstra’s search with $\mathbf{X}_{inlet} = [0, 0 : 800]$. Yellow colouring is a high likelihood whilst blue colouring is a low likelihood.

Since the Entrotaxis approach is the fundamental basis of the motion planner, this forms the benchmark from which to draw conclusions about the proposed algorithm. To ensure functionality in a feature rich environment, Entrotaxis is slightly modified for simple obstacle avoidance, so that any candidate trajectories $\sigma \subseteq \mathbf{X}_{obs}$ are discarded before utility calculation.

This paper presents two unique additions to the source search process: informed tree search and sample generation. To prove the efficacy of the sample generation methodology, the system is also tested without this feature (dubbed uniform tree search) and compared alongside the fully informed tree search algorithm.

7.1 Test Setup

Each control strategy is tested across all 3 sources with the same prior parameters of Θ initiated for each source, as shown in Table 1. Testing three sources ensures that results can be evaluated for their general optimality, as opposed to the circumstance that a particular method favours a single type of source release.

To further test adaptability of the proposed algorithm, 4 starting locations are also tested for each source (shown in Fig. 6). Locations 1, 2, 3 & 4 are situated at $[1100,50]$, $[100,50]$, $[100,650]$ & $[1100,650]$ respectively. Location 1 replicates the condition that the agent is deployed downwind of the plume and at the boundary of recordable concentrations. This location is the most ideal scenario as the robot is likely to get information about the source immediately and therefore should be able to localise quickly (particularly for source 3). Location 2 represents the agent starting in an upwind position and therefore it is unlikely to record positive data during the initial phase. However, all 3 sources lie within a direct line to $\mathbb{E}(\theta_x^{(1)})$ and therefore the robot has a chance of sampling high concentration areas later on. Location 3 is upwind and the opposite quadrant to the majority of the plume structure. This is hypothetically the most challenging start location from which to resolve the sources (particularly source 3). Location 4 is located downwind but outside of the main structure of the plumes. 20 repeats are performed for each location, leading to 240 simulations per control method. This equates to 30 days of continuous real-world testing which ensures reliability of the conclusions drawn.

Model parameters for the estimation engine are shown in Table 1 alongside the ground truth values of the sources. Sources 1, 2, & 3 locations are $[455, 370]$, $[475, 376]$ & $[534, 300]$ respectively.

Parameters for the Entrotaxis, Uniform tree search and Informed tree search are outlined in Table 2. To ensure a fair comparison, all three control methods are subject to the same number of utility calculations per step (equating to $|\Sigma|$), and the predictive measurements of the particle filter n_z also remains constant. From the obstacle map of the DAPPLE domain, the sample generation distribution for the informed tree search is shown in Fig. 6.

To model the sampling robot, we assume a simple unmanned ground/aerial vehicle with parameters outlined in Table 3. The vehicle is fitted with a single fast response chemical sensor capable of detecting down to a minimum concentration of $0.1\text{g}/\text{m}^3$. Due to the limitations of the dataset, concentration data is only available at a sampling height of 5m and

Table 1: Model parameters for the estimation engine prior parameters alongside ground truth values.

| Model Parameters | Ground Truth | Initial Prior |
|----------------------------|-------------------------|-------------------------|
| x position x_s | source _{1,2,3} | $\mathcal{N}(600, 150)$ |
| y position y_s | source _{1,2,3} | $\mathcal{N}(400, 150)$ |
| z position z_s | 0m | $\mathcal{N}(1, 0.5)$ |
| Release rate q_s | 310, 260, 23 mg/s | $\gamma(2, 1)$ |
| Wind speed u_s | 2.5m/s | $\mathcal{N}(2.5, 2)$ |
| Wind direction ϕ_s | 270° | $\mathcal{N}(270, 10)$ |
| Diffusivity d_s | — | $\mathcal{N}(1, 2)$ |
| Particle lifetime τ_s | — | $\mathcal{N}(8, 2)$ |
| PF Particles n | - | 20,000 |
| Effective ratio η | - | 0.5 |

Table 2: Parameters for IPP

| Operational Parameters | Robot |
|--------------------------------|---|
| Number of nodes, N | 4000 |
| Goal set neighbours, k_n | 5 |
| Sample evaluations, $ \Sigma $ | 24 |
| Entrotaxis step size | [10,20]m |
| Entrotaxis step directions | $[0^\circ, 45^\circ, \dots, 315^\circ]$ |
| Predictive measurements, n_z | 40 |

Table 3: Operational parameters for simulated robot

| Operational Parameters | Robot |
|------------------------|---------------------|
| Motion Model | constant velocity |
| Velocity | 2m/s |
| Time budget | 3600s |
| Sensor threshold | 10mg/m ³ |
| Sampling altitude | 5m |

therefore it is assumed that the robot has a fixed sampling height. To model motion, a constant velocity model of the robot is used. The time budget allowed is more conducive to a ground vehicle however, conclusions for suitability on a UAV can still be drawn by analysing the presented results at a lower time budget.

7.2 Results

To analyse the performance of a searching strategy, the weighted root mean square error (RMSE) between the source location $\mathbf{s}_{x,y}$ and the current posterior estimate of the Bayesian inference $\theta_x^{(k)}$ is recorded after each sampling event. The equation for calculating weighted RMSE is:

$$RMSE_k = \sqrt{\sum_{i=1}^n \mathbf{w}_k^{(i)} (\theta_x^{(k)} - \mathbf{s})^2} \quad (6)$$

7.2.1 Overall evaluation

Fig. 7 shows the average RMSE at each time step, as well as 1σ upper and lower bounds of the 240 runs per method. It is clear to see that both the uniform and informed tree search show significant improvement over the standard Entrotaxis approach. Both uniform and informed searches show a much greater initial rate of error reduction and well as having a better average final RMSE at $k = 3600$ s (40m vs 60m). Furthermore, the variance of the proposed methods are much narrower than Entrotaxis, showing that performing the tree search gives significantly more consistent results than with Entrotaxis.

The uniform and informed tree searches are both tested against each other in order to ascertain the benefit of performing a tree search based on the likely particle trajectory in wind. There is a clear gain that can be seen with the informed method, particularly regarding the initial rate of error reduction (although this gain is not as significant as using tree search over the myopic approach). It can also be seen that final RMSE for informed tree search is smaller with less

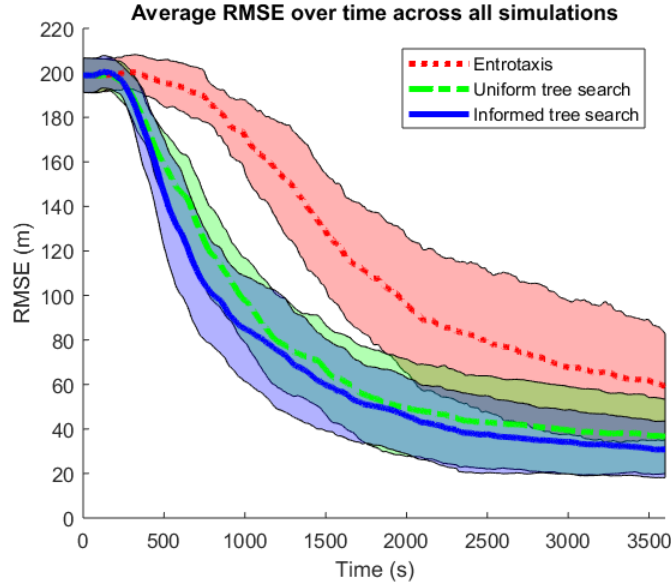


Figure 7: RMSE over time averaged across all 240 Monte Carlo simulations and compared for each control method. 1 standard deviation bounds from the mean are shown in the corresponding mean line colour.

variance. Therefore, it can be concluded that applying the sample generation technique gives an efficiency bonus when trying to reduce source estimate error, which is a key contribution when considering a sampling agent with a limited operational budget.

7.2.2 Starting location evaluation

As outlined in the simulation setup, the 4 different start locations challenge the search algorithms in different ways. In Fig. 8, a box plot is shown that isolates out the final RMSE data for each starting location. From this graph, the range of convergence across locations can be assessed as well as the relative convergent performance between methods. Entrotaxis can clearly be shown to have a larger interquartile range (IQR) than the tree searches as well as having more variability between IQRs based on position. This leads to the conclusion that Entrotaxis is more reliant on the starting conditions in this urban environment to get consistent results. For example, starting position 1 of Entrotaxis shows the most consistency (smallest IQR) due to the robot starting downwind and at the plume boundary, whereas positions 3 & 4 (upwind positions) show the greatest inconsistency which implies Entrotaxis struggles more in upwind starting conditions that are away from the plume. Contrary to this, both tree searches have extremely consistent IQRs across the starting positions which indicates that the tree search procedure is much more robust to differing initial conditions. This is a key property when considering an autonomous platform operating in an unknown environment. Furthermore, the final difference between the informed search and the uniform search is marginal, which is to be expected since it has been determined that the sample generation technique should only allow more efficient trajectories to be taken, rather than dictating the final performance of source term estimation.

For context, example trajectories for a single run of the informed tree search and Entrotaxis are shown in Fig. 9. The efficiency bonus of using informed trees is clear to see as 1800s into the simulation the informed tree approach has navigated the robot to the vicinity of the source location, whereas Entrotaxis has not reached the main plume.

8 Conclusion

In this paper, we attempt to integrate obstacle avoidance trajectory generation with a source term estimation engine to create efficient sampling trajectories through an urban environment. By combining a state-of-the-art parametric inference model alongside a single batch informed tree search algorithm, we are able to efficiently navigate a sampling robot in an informed manner towards a source location. Furthermore, local minima are avoided by taking exploratory actions relative to the uncertainty of the source location estimate. As demonstrated in the simulation studies, the presented approach is reliably capable of localising a source within a large scale feature rich environment from a variety of different source terms and varied start conditions. The informed tree search is shown to far outperform Entrotaxis in

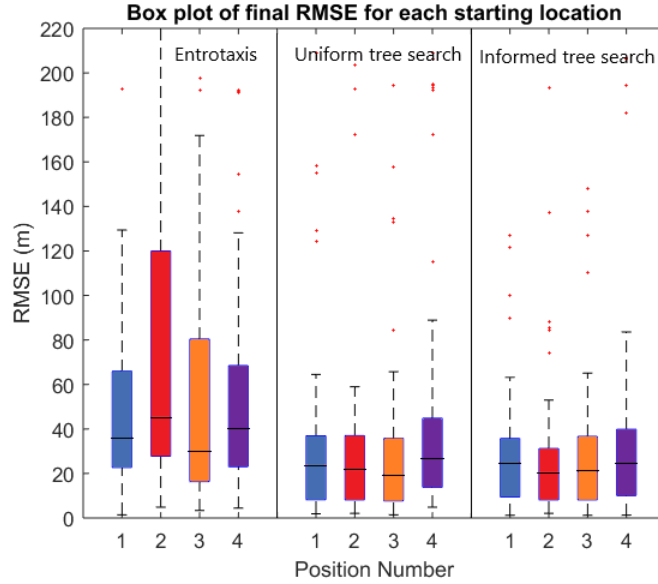


Figure 8: Boxplot of the RMSE at $k = 3600s$ for each starting location compared across control methods. Starting position numbers refer to locations in Fig. 6.

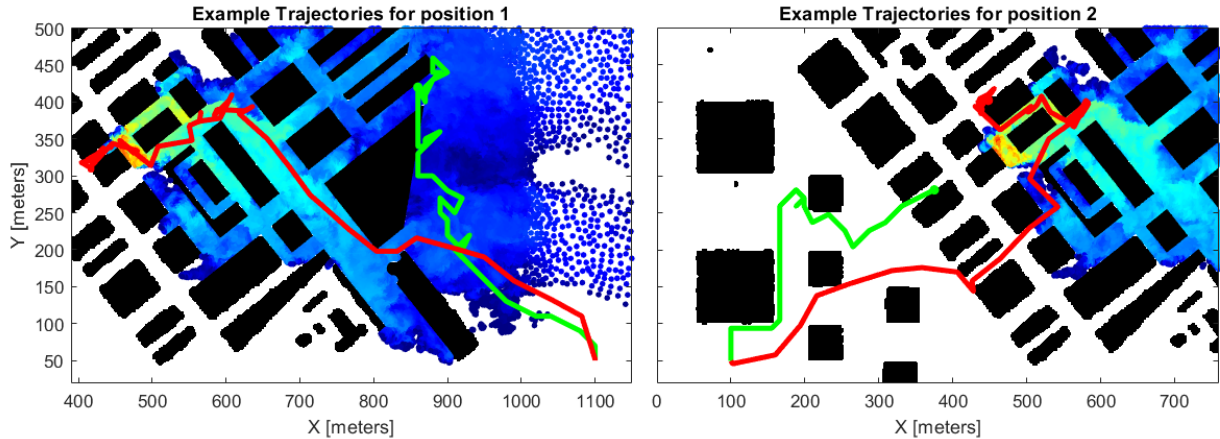


Figure 9: Example trajectories for estimating source 1 with starting positions 1 & 2 from $t = 0$ to $t = 1800s$ of simulation time. Red line indicates the informed tree historic trajectory and green line represents the Entrotaxis trajectory.

an urban environment when evaluating the same number of possible future sampling locations, proving the efficiency bonus of planning trajectories towards the goal. The addition of an informed sample generation algorithm, as opposed to a uniform distribution, is also shown to provide a further efficiency bonus with regards to the rate of error reduction that can be achieved. The results demonstrate that the proposed framework is capable of guiding sensing robots to respond to emergency CBRN events in urban environments.

Acknowledgements

The author would like to thank the Engineering and Physical Sciences Research Council (EPSRC) for their support under award 2126619 and Tim Foat at the Defence Science and Technology Laboratory (DSTL) for providing the DAPPLE experiment dataset used as the ground truth in this paper.

References

- Robin R. Murphy, Joshua Peschel, Clint Arnett, and David Martin. Projected needs for robot-assisted chemical, biological, radiological, or nuclear (CBRN) incidents. *2012 IEEE International Symposium on Safety, Security, and Rescue Robotics, SSRR 2012*, 00(c):1–4, 2012. doi:10.1109/SSRR.2012.6523881.
- Ioannis Tsitsimpelis, C. James Taylor, Barry Lennox, and Malcolm J. Joyce. A review of ground-based robotic systems for the characterization of nuclear environments. *Progress in Nuclear Energy*, 111(October 2018):109–124, 2019. ISSN 01491970. doi:10.1016/j.pnucene.2018.10.023. URL <https://doi.org/10.1016/j.pnucene.2018.10.023>.
- Branko Ristic, Alex Skvortsov, and Ajith Gunatilaka. A study of cognitive strategies for an autonomous search. *Information Fusion*, 28:1–9, 2016. ISSN 1566-2535. doi:<https://doi.org/10.1016/j.inffus.2015.06.008>. URL <https://www.sciencedirect.com/science/article/pii/S1566253515000597>.
- Lucas Janson, Edward Schmerling, Ashley Clark, and Marco Pavone. Fast marching tree: A fast marching sampling-based method for optimal motion planning in many dimensions. *International Journal of Robotics Research*, 34(7):883–921, 2015. ISSN 17413176. doi:10.1177/0278364915577958.
- Jonathan D. Gammell, Siddhartha S. Srinivasa, and Timothy D. Barfoot. Batch Informed Trees (BIT): Sampling-based optimal planning via the heuristically guided search of implicit random geometric graphs. *Proceedings - IEEE International Conference on Robotics and Automation*, 2015-June(June):3067–3074, 2015. ISSN 10504729. doi:10.1109/ICRA.2015.7139620.
- Wen Hua Chen, Callum Rhodes, and Cunjia Liu. Dual Control for Exploitation and Exploration (DCEE) in Autonomous Search. *preprint*, 2020. URL <http://arxiv.org/abs/2012.06276>.
- Javier Monroy and Javier Gonzalez-Jimenez. Towards Odor-Sensitive Mobile Robots. *Rapid Automation*, pages 1491–1510, 2019. doi:10.4018/978-1-5225-8060-7.ch070.
- Chaoqun Wang, Teng Li, Max Q.-H. Meng, and Clarence De Silva. Efficient Mobile Robot Exploration with Gaussian Markov Random Fields in 3D Environments. *2018 IEEE International Conference on Robotics and Automation (ICRA)*, pages 5015–5021, 2018. doi:10.1109/icra.2018.8460788.
- Massimo Vergassola, Emmanuel Villerman, and Boris I. Shraiman. ‘Infotaxis’ as a strategy for searching without gradients. *Nature*, 445(7126):406–409, 2007. ISSN 14764687. doi:10.1038/nature05464.
- Michael Hutchinson, Pawel Ladosz, Cunjia Liu, and Wen Hua Chen. Experimental assessment of plume mapping using point measurements from unmanned vehicles. In *Proceedings - IEEE International Conference on Robotics and Automation*, volume 2019-May, pages 7720–7726, 2019a. ISBN 9781538660263. doi:10.1109/ICRA.2019.8793848.
- Achim J. Lilienthal, Matteo Reggente, Marco Trinca, Jose Luis Blanco, and Javier Gonzalez. A statistical approach to gas distribution modelling with mobile robots - The Kernel DM+V algorithm. *2009 IEEE/RSJ International Conference on Intelligent Robots and Systems, IROS 2009*, pages 570–576, 2009. doi:10.1109/IROS.2009.5354304.
- Javier G. Monroy, Jose Luis Blanco, and Javier Gonzalez-Jimenez. Time-variant gas distribution mapping with obstacle information. *Autonomous Robots*, 40(1):1–16, 2016. ISSN 15737527. doi:10.1007/s10514-015-9437-0.
- Andres Gongora, Javier Monroy, and Javier Gonzalez-Jimenez. Joint Estimation of Gas & Wind Maps for Fast-Response Applications. *Applied Mathematical Modelling*, 87:655–674, 2020. ISSN 0307904X. doi:10.1016/j.apm.2020.06.026.
- Sahar Asadi, Han Fan, Victor Hernandez Bennetts, and Achim J. Lilienthal. Time-dependent gas distribution modelling. *Robotics and Autonomous Systems*, 96:157–170, 2017. ISSN 09218890. doi:10.1016/j.robot.2017.05.012. URL <http://dx.doi.org/10.1016/j.robot.2017.05.012>.
- Callum Rhodes, Cunjia Liu, and Wen-hua Chen. Informative Path Planning for Gas Distribution Mapping in Cluttered Environments *. In *2020 IEEE/RSJ International Conference on Intelligent Robots and Systems (IROS)*, pages 6726–6732, 2020. doi:10.1109/IROS45743.2020.
- Vadiraj Hombal, Arthur Sanderson, and D. Richard Blidberg. Multiscale adaptive sampling in environmental robotics. *IEEE International Conference on Multisensor Fusion and Integration for Intelligent Systems*, pages 80–87, 2010. doi:10.1109/MFI.2010.5604463.
- Enric Galceran and Marc Carreras. A survey on coverage path planning for robotics. *Robotics and Autonomous Systems*, 61(12):1258–1276, 2013. ISSN 09218890. doi:10.1016/j.robot.2013.09.004. URL <http://dx.doi.org/10.1016/j.robot.2013.09.004>.
- David J. Harvey, Tien Fu Lu, and Michael A. Keller. Comparing insect-inspired chemical plume tracking algorithms using a mobile robot. *IEEE Transactions on Robotics*, 24(2):307–317, 2008. ISSN 15523098. doi:10.1109/TRO.2007.912090.

- Amit Dhariwal, Gaurav S. Sukhatme, and Aristides A.G. Requicha. Bacterium-inspired robots for environmental monitoring. *Proceedings - IEEE International Conference on Robotics and Automation*, 2004(2):1436–1443, 2004. ISSN 10504729. doi:10.1109/robot.2004.1308026.
- R. Andrew Russell, Alireza Bab-Hadiashar, Rod L. Shepherd, and Gordon G. Wallace. A comparison of reactive robot chemotaxis algorithms. *Robotics and Autonomous Systems*, 45(2):83–97, 2003. ISSN 09218890. doi:10.1016/S0921-8890(03)00120-9.
- Ali Marjovi and Lino Marques. Optimal swarm formation for odor plume finding. *IEEE Transactions on Cybernetics*, 44(12):2302–2315, 2014. ISSN 21682267. doi:10.1109/TCYB.2014.2306291.
- Jatmiko Wisnu, Sekiyama Kosuke, and Fukuda Toshio. A PSO-Based Mobile Robot for Odor Source Localization in Dynamic Advection-Diffusion with Obstacles Environment: Theory, Simulation and Measurement. *IEEE Computational Intelligence Magazine*, pages 37–51, 2007.
- Michael Hutchinson, Hyondong Oh, and Wen Hua Chen. Entrotaxis as a strategy for autonomous search and source reconstruction in turbulent conditions. *Information Fusion*, 42(March 2017):179–189, 2018. ISSN 15662535. doi:10.1016/j.inffus.2017.10.009. URL <https://doi.org/10.1016/j.inffus.2017.10.009>.
- Nicole Voges, Antoine Chaffiol, Philippe Lucas, and Dominique Martinez. Reactive Searching and Infotaxis in Odor Source Localization. *PLoS Computational Biology*, 10(10), 2014. ISSN 15537358. doi:10.1371/journal.pcbi.1003861.
- Michael Hutchinson, Cunjia Liu, and Wen Hua Chen. Information-Based Search for an Atmospheric Release Using a Mobile Robot: Algorithm and Experiments. *IEEE Transactions on Control Systems Technology*, 27(6):2388–2402, 2019b. ISSN 15580865. doi:10.1109/TCST.2018.2860548.
- Michael Hutchinson, Cunjia Liu, Paul Thomas, and Wen Hua Chen. Unmanned Aerial Vehicle-Based Hazardous Materials Response: Information-Theoretic Hazardous Source Search and Reconstruction. *IEEE Robotics and Automation Magazine*, (March 2019):1–11, 2019c. ISSN 1558223X. doi:10.1109/MRA.2019.2943006.
- Lukas Schmid, Michael Pantic, Raghav Khanna, Lionel Ott, Roland Siegwart, and Juan Nieto. An Efficient Sampling-Based Method for Online Informative Path Planning in Unknown Environments. *IEEE Robotics and Automation Letters*, 5(2):1500–1507, 2020.
- Ali Marjovi and Lino Marques. Multi-robot olfactory search in structured environments. *Robotics and Autonomous Systems*, 59(11):867–881, 2011. ISSN 09218890. doi:10.1016/j.robot.2011.07.010. URL <http://dx.doi.org/10.1016/j.robot.2011.07.010>.
- Yong Zhao, Bin Chen, Zhengqiu Zhu, Feiran Chen, Yiduo Wang, and Denglong Ma. Entrotaxis-Jump as a hybrid search algorithm for seeking an unknown emission source in a large-scale area with road network constraint. *Expert Systems with Applications*, 157(May):113484, 2020. ISSN 09574174. doi:10.1016/j.eswa.2020.113484. URL <https://doi.org/10.1016/j.eswa.2020.113484>.
- Sertac Karaman and Emilio Frazzoli. Sampling-based Algorithms for Optimal Motion Planning. *The International Journal of Robotics Research*, 30(7):846–894, 2011. ISSN 0278-3649. doi:10.1177/0278364911406761. URL <http://arxiv.org/abs/1105.1186>.
- John Bellingham, Arthur Richards, and Jonathan P. How. Receding horizon control of autonomous aerial vehicles. *Proceedings of the American Control Conference*, 5(April 2014):3741–3746, 2002. ISSN 07431619. doi:10.1109/ACC.2002.1024509.
- D. Martin, G. Nickless, C. S. Price, R. E. Britter, M. K. Neophytou, H. Cheng, A. G. Robins, A. Dobre, S. E. Belcher, J. F. Barlow, A. S. Tomlin, R. J. Smalley, J. E. Tate, R. N. Colvile, S. J. Arnold, and D. E. Shallcross. Urban tracer dispersion experiment in London (DAPPLE) 2003: Field study and comparison with empirical prediction. *Atmospheric Science Letters*, 11(4):241–248, 2010. ISSN 1530261X. doi:10.1002/asl.282.